IMPROVEMENT IN CODED-APERTURE IMAGE QUALITY USING CONTINUOUS MASK ROTATION

Steven T. Brown, Reid Sobota, David I. Goodman, James R. Mason, David Tefft
H3D, Inc., Ann Arbor, MI, 48108 US

Ammon N. Williams, Janine N. Lambert, David L. Chichester
Idaho National Laboratory, Idaho Falls, ID, 83415 US

ABSTRACT

Holdup is the residual nuclear material inside process equipment at nuclear facilities and it is routinely measured for materials accounting and criticality safety. However, quantitative material estimates derived from these measurements are subject to significant error due to the unknown distribution of material inside. Although not widely used, portable gamma cameras are useful tools for this application because they can resolve the location and shape of nuclear materials, potentially providing material quantities directly from the image. Coded-aperture imagers can efficiently image low-energy gamma emissions with high resolution and the ideal response is a delta-function. However, the measured response is generally nonuniform and subject to irregularities that can significantly bias the result. Traditional coded-aperture masks are static during a measurement, or switch discretely between mask and antimask configurations, but continuous motion has been shown to significantly increase image SNR by averaging out image artifacts. In this work, we investigate the use of continuous mask rotation for the H420, a commercial CZT-based imager. A two-fold improvement in point-source SNR was shown for continuous rotation versus conventional mask-antimask switching. Results for both MURA- and HURA-based mask patterns are reported along with images of several HEU samples.

INTRODUCTION

The H420 imaging spectrometer is a commercial gamma camera with a coded aperture mask that periodically switches between mask and antimask configurations to subtract background [1]. Because the mask must rotate to move between states, the mechanical parts are already in place for continuous rotation. Rotation can mitigate ambiguities introduced by repeating uniformly-redundant-array (URA) patterns [2] and has potential to improve image signal-to-noise ratio (SNR). For example, scanning through the entire mask pattern in two dimensions has been shown to improve point-source SNR by an order of magnitude by averaging out nonuniform detector response [3, 4]. Unfortunately, this type of motion introduces mechanical complexity that is poorly suited for handheld imagers. But simple rotation of a planar mask may only require a DC motor, a belt, and a sensor to count revolutions.

This work investigates the effect of continuous mask rotation on H420 coded-aperture image quality. Higher image SNR can enable more accurate quantitative imaging for applications such as holdup measurements [5, 6]. In this work, a hexagonal-URA (HURA) mask was designed and fabricated to compare to the standard modified-URA (MURA) mask. Its circular shape was expected to be more amenable to measurement while rotating. Simulations were done to predict

improvements in image SNR and two low-energy check sources were measured to verify the findings. Several highly enriched uranium (HEU) sources were also measured in continuous and switching modes for direct comparison.

METHODS

Mask Design and Fabrication

The commercial H420's mask consists of an array of square tungsten tiles arranged in a modified uniformly redundant array (MURA) [1]. Each tile is 1.5-mm thick and about 2.1-mm across. The rank-19 MURA pattern is 50% open and antisymmetric upon 90º rotation. A 3D-printed plastic substrate with an array of small pockets holds the tiles in place. The substrate is circular to allow rotation between mask and antimask configurations using a belt and motor. The stepper motor beings moving at the start of a measurement and stops when an optical sensor arrives at one of four tabs separated by 90º on the inner lip of the mask. During a measurement, the mask is set to switch between mask and antimask configurations every 60 seconds. Behind the mask, a 2 by 2 array of pixelated CZT crystals measures the modulated gammas. The detectors have about 1% FWHM energy resolution at 662 keV with sub-mm position resolution [1].

A software change was made to allow the H420 to measure during continuous mask rotation. Rather than pause at each quadrant, the position of the mask was linearly interpolated between the four tab positions detected by the optical sensor as it moved past. A different mask pattern based on a hexagonal grid was also selected. The hexagonal uniformly redundant array (HURA) has a flat-sidelobe response like the MURA as well as mask-antimask background cancellation. A side-by-side picture of the two basic patterns is shown in Figure 1. The near-circular shape of the HURA was expected to be better for rotation. For example, when the MURA is tilted at 45 degrees, the corners of the pattern are beyond the extent of the square detector array, so only a partial pattern would be recorded.

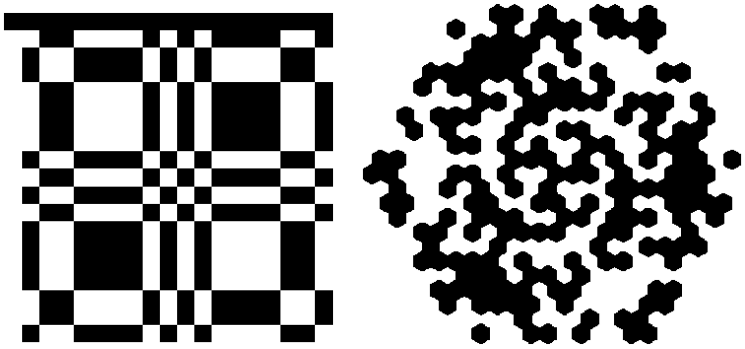

Figure 1: (Left) 361-element MURA base pattern used in the commercial H420 imager. (Right) 367-element HURA base pattern chosen for the continuously rotating H420 mask.

Figure 2 shows the fabricated HURA-based mask with plastic substrate. Each tile is hexagonal with same thickness and pitch (from flat to flat) as the H420's MURA mask. The pattern was positioned to preserve its antisymmetry and repeated to fill a circular area with diameter of about 95 mm. The mask was installed into an H420 for comparison to a MURA mask on another H420.

Figure 2: Renderings of prototype with scanning mask in down and up positions.

Simulation and Image Reconstruction

A simple ray-tracing simulation script was written in MATLAB to simulate the coded-aperture imaging process in an idealized manner. No scattering was considered; only rays between image pixels to the CZT detector, both represented by planar grids of points in 3D. The detector was modeled as a 2 by 2 surface that matched the footprint of the CZT sensitive area inside the H420. Including dead regions near the CZT edge and a small gap between crystals, the effective gap between neighboring detectors was about 1.5 mm wide. The 11 by 11 pixels on each of the CZT was divided into 3 by 3 subpixels, roughly matching the position resolution of the CZT. Aside from the gap, the simulated detectors had an idealized, uniform response.

The mask plane consisted of one or more layers of attenuating elements that either stop or let signal through. Both hexagonal and square-shaped mask elements were modeled to represent the MURA and HURA patterns. Rotation of the mask was approximated by discrete, 1º steps. To calculate the image of a point source, rays were projected from a point on the image plane onto the gridded detector surface and modulated by the mask. The recorded counts were then projected back to the image plane through the mask. Weights were applied during back projection according to detector location to ensure optimal sampling of the MURA and HURA patterns at each step during rotation [7]. This process was repeated and summed for each sampled angle of the mask. This image reconstruction algorithm is typically referred to as simple back projection (SBP) and was used to form images from both simulated and measured data in this work. It is also used by H3D's commercial imaging software.

A series of point-source images were calculated using the simulation code to quantify image SNR. The source was positioned in 10-cm steps between 10 and 100 cm from the mask and at six lateral positions, stepping from FOV center towards the corner. Signal-to-noise ratio was defined for a point source as

$$SNR = \frac{I_{max} - \mu_o}{\sigma_o}, \quad (1)$$

where I_{max} is the maximum image pixel value and μ_o and σ_o are the mean and standard deviation of the image pixels outside the hotspot ROI. The hotspot ROI was defined as a square region with

side length 2.5 times the hotspot FWHM. This formula was used to observe the relative difference in SNR between HURA and MURA masks, with and without rotation. Because detector nonuniformities were not modeled, the magnitude of the SNR from these simulations is expected to represent the best-case scenario for an ideal detector and mask in the H420 configuration.

Experimental Tests

To experimentally measure the gain in SNR gained from rotation, Co-57 and Ho-166m check sources were imaged by H420s in both switching and rotating modes. One of the imagers used a HURA mask and the other a MURA. The sources were positioned one at a time near the center of each imager's FOV, about 50 cm from their masks. Energy windows around the 122-keV and 184-keV photopeaks were used for each respective isotope, which were measured until statistical convergence, on the order of 10^5 counts.

The imagers also measured five HEU samples for a test that was more representative of holdup measurements at US nuclear facilities. These samples were sealed inside cans and had chemical form U_3O_8. The configuration of materials inside the cans was unknown prior to the measurement, but each had a label indicating the total mass and U-235 enrichment. From the perspective of Figure 3, all cans contained 25 g U except for the top left can (tallest), which contained 29 g. From left to right and top to bottom, the U-235 enrichments were 11.77%, 21%, 26.84%, 51.58%, and 37.70%.

The H420s containing the HURA and MURA masks were positioned 50 cm from the can's centerline on opposite sides. A third H420 with a MURA mask and a high-resolution imager developed by the Defense Threat Reduction Agency (DTRA) were also used for comparison. The high-resolution imager can reach an order-of-magnitude higher SNR than the H420 [4]. The samples were measured in switching and continuous mode for 2.25 h each while the high-resolution imager measured for 4.5 h total.

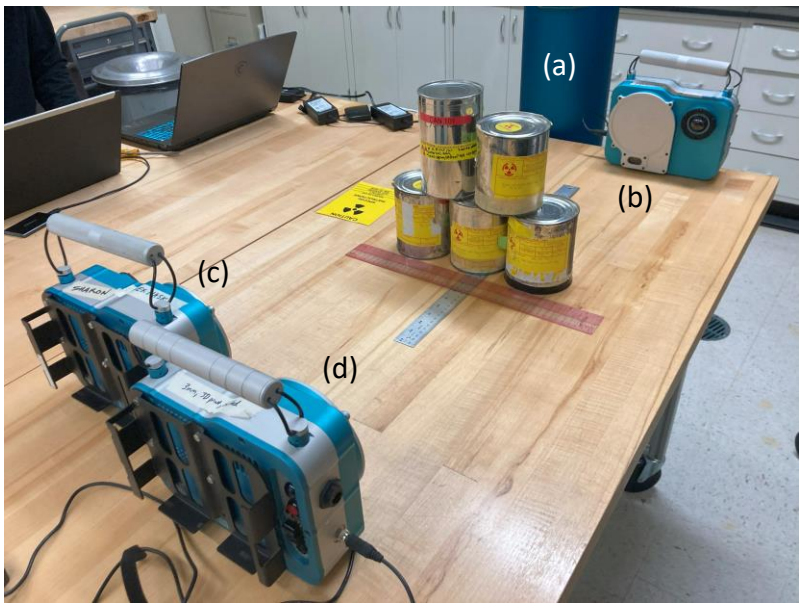

Figure 3: Photo of (a) a high-resolution imager and (b-d) three H420 imagers measuring uranium samples inside cans. Imagers (b) and (d) used a MURA mask while (c) used a HURA.

RESULTS

The plot of Figure 4 shows the results from ray-tracing simulation. The curve indicates that a source must be at least 30 cm from the mask to avoid overmagnification, which is consistent with the focal length of the H420. Beyond that distance, the SNR is roughly constant. In this idealized simulation, the rotating masks reached between 100% to 200% higher SNR compared to standard mask-antimask switching. The simulations also predicted a relatively small (~25%) advantage for the HURA compared to the MURA masks on average.

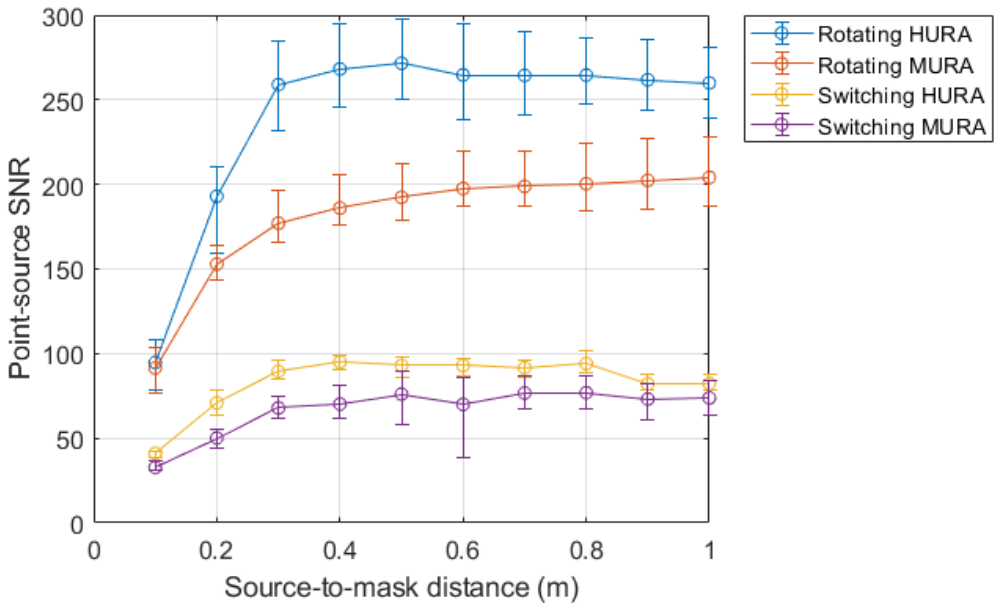

Figure 4: Simulated SNRs vs. distance for switching and rotating masks. Error bars mark the full range of SNRs for six positions within the FOV and each circular marker is the mean.

Measured results of Table 1 show a smaller, but still significant increase point-source SNR for mask rotation over mask-antimask switching. Signal-to-noise ratio increased by 55% and 100% for the MURA and HURA masks, respectively. Although simulation predicted about the same boost in SNR for the two masks, they cannot be directly compared because they were paired with different detectors. Figure 5 shows the Ho-166m images from the switching MURA, or the standard H420, and the HURA with continuous rotation. A horizontal cross section through the hotspot is also shown, showing flatter sidelobes for the rotating mask.

Table 1: Measured SNRs for switching vs. rotating masks.

Pattern	Source	Switching SNR	Rotating SNR
MURA	Ho-166m	57	88
HURA	Ho-166m	50	98
HURA	Co-57	47	90

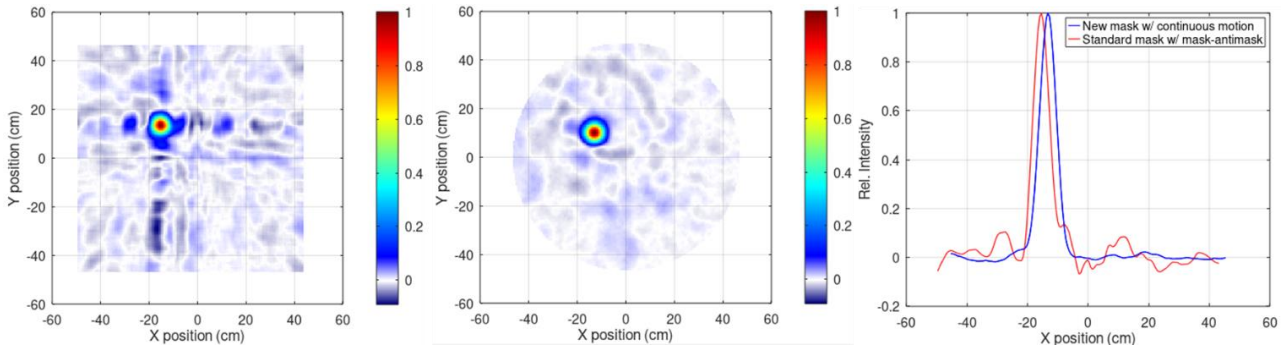

Figure 5: Images of Ho-166m with a color scale that highlights background noise in the image. (Left) MURA mask in switching mode. (Center) HURA mask in rotating mode. (Right) Horizontal cross section through the hotspot of each image.

Figure 6 shows the results from imaging the HEU cans of various enrichment with rotating and switching HURA masks. The low end of the MATLAB "jet" color scale in each image was automatically adjusted so that the transition of low-intensity dark blue to cyan occurs at 5-sigma above the background noise. Hence, only sources that are statistically significant appear as cyan or above on the color scale. A similar algorithm is used to set a noise threshold for optical image overlay for H3D's commercial imaging software. The figure shows that the relatively weak sources A and B appeared above the noise for the rotating measurement but not switching. Source B was confirmed to be a deposit of HEU material near the top of the can, possibly on the internal packaging of the 51.58%-enriched source. The MURA mask of Figure 7 also shows a small but visually noticeable improvement in image SNR, also revealing source B from the opposite side of the can. Figure 8 shows the clearest image of the objects using the high-resolution imager, again confirming the presence of the weaker sources A and B.

Figure 9 plots the relative intensity of each hotspot in Figure 7 and Figure 8 corrected for solid angle, showing a roughly linear trend with HEU enrichment. The linear estimate is based on the material label on each can with the assumption of isotropic emission. Note this is not exactly true due to self-attenuation of the U_3O_8 material. Note that there was better agreement between the high-resolution imager and the H420 when the H420's mask was rotating. The RMS error between the two sets of datapoints was reduced by roughly a factor of two for the rotating case. The corresponding estimates from the two H420s on the opposite side of the cans, or c) and d) in Figure 3, were also reduced by about a factor of two when they were set to rotating mode instead of switching.

CONCLUSIONS

The commercial H420 coded-aperture imager was tested in mask-antimask switching and continuous rotation modes to evaluate the improvement in image quality. Increases in point-source SNRs of 55% and 100% were measured for MURA- and HURA-patterned masks, respectively. Images of complex HEU sources were also acquired in both modes, showing a noticeable improvement in image quality with rotation. Intensities of HEU sources corresponded well to relative image intensities, which showed better agreement using mask rotation when compared to a reference detector. The continuous-mode H420 will be studied further to evaluate its performance for quantitative imaging for holdup and other measurements.

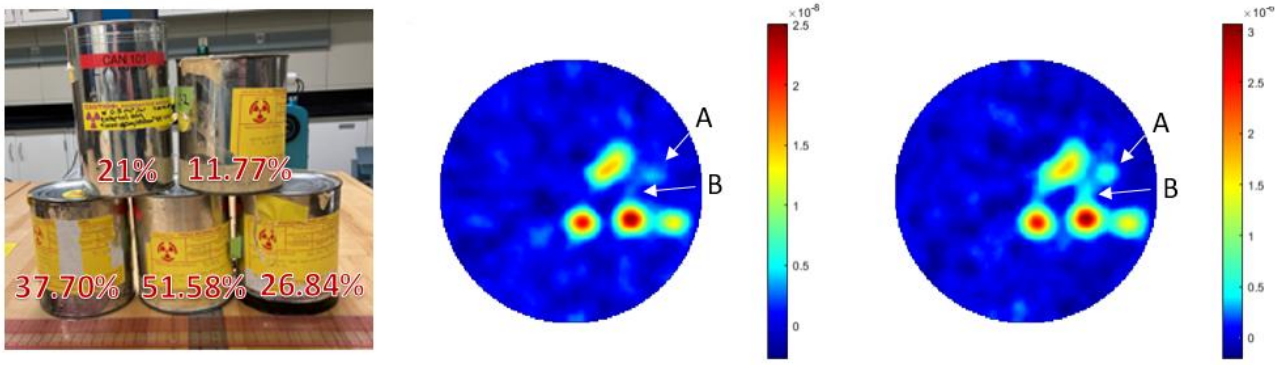

Figure 6: (Left) Stacked cans of U_3O_8 of various enrichment measured by the H420 with HURA mask. (Center) Image formed with mask in switching mode. (Right) Image formed with mask in rotating mode. Two weak hotspots A and B are marked and discussed in the text.

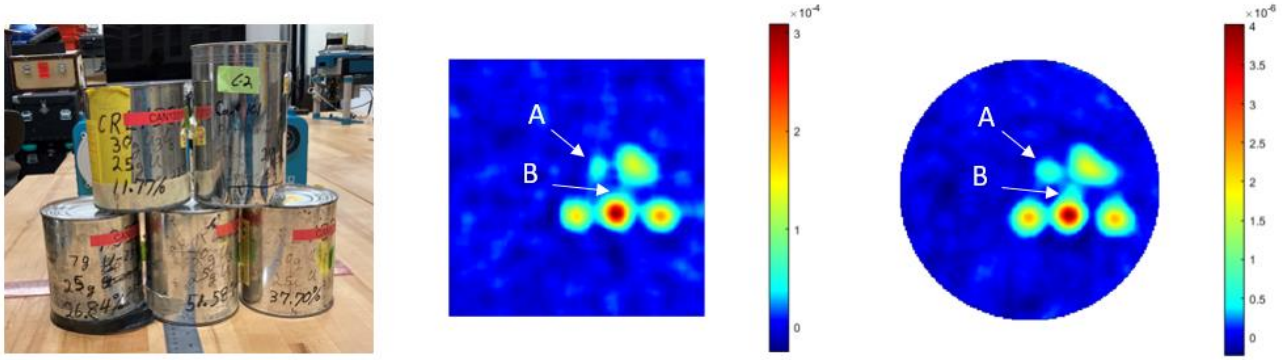

Figure 7: (Left) Opposite view of HEU cans from Figure 6 measured by an H420 with MURA mask. (Center) Image formed with mask in switching mode. (Right) Image formed with mask in rotating mode.

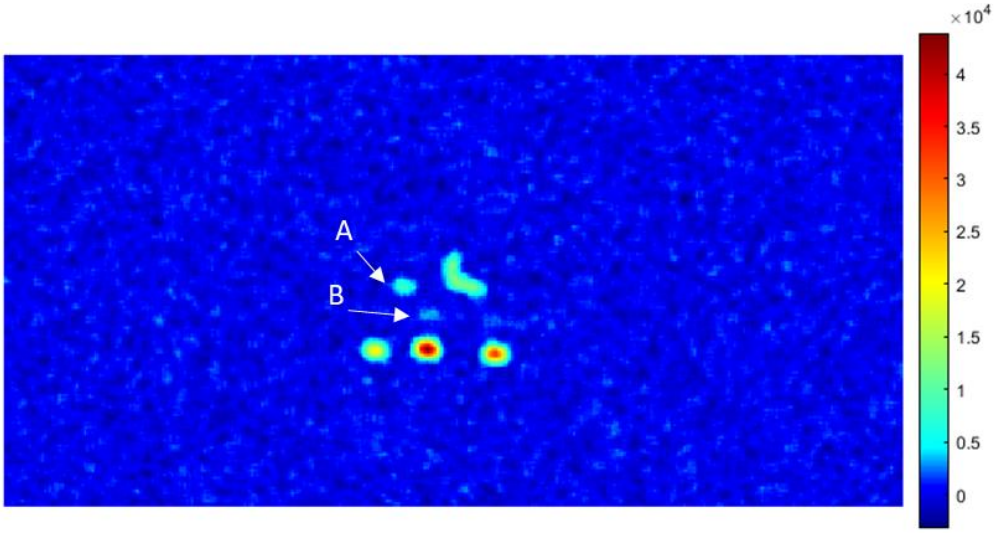

Figure 8: Image of the HEU cans from the high-resolution imager [4].

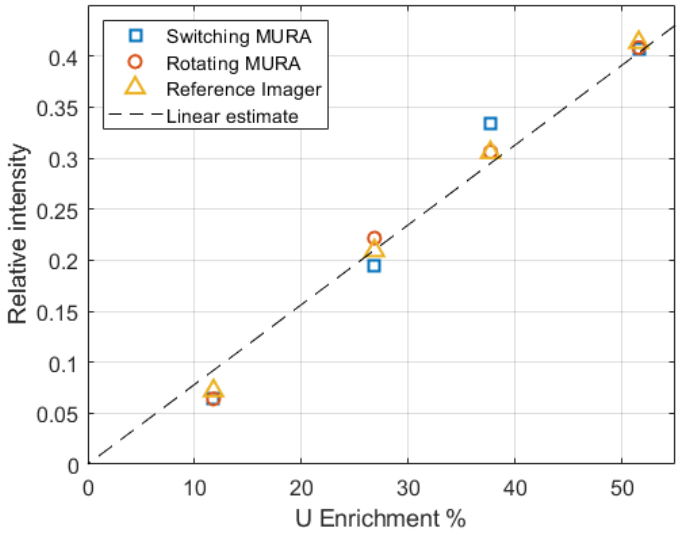

Figure 9: Relative intensity of each hotspot in Figure 7 and Figure 8 corrected for solid angle and plotted against HEU enrichment (each sample had equal mass).

ACKNOLWEDGEMENTS

The authors would like to thank the staff at Idaho National Laboratory for hosting the measurements of special nuclear materials. The high-resolution imager was lent to H3D by DTRA. This material is based upon work supported by the U.S. Department of Energy, Office of Science, under Award Number DE-SC0021768.

REFERENCES

[1] Wahl, C. G., et al. "Coded-aperture imaging with high-resolution large-volume CZT." *2018 IEEE Nuclear Science Symposium and Medical Imaging Conference Proceedings*, 2018.

[2] Cook, W. R., et al. "Gamma-ray imaging with a rotating hexagonal uniformly redundant array." *IEEE Transactions on Nuclear Science* 31.1 (1984): 771-775.

[3] Grindlay, J. E., and Hong, J. " Optimizing wide-field coded aperture imaging: radial mask holes and scanning. " *Optics for EUV, X-Ray, and Gamma-Ray Astronomy* 5168 (2004): 402-410.

[4] Brown, S. T., et al. "A Scanning Coded-Aperture Imager for Nuclear and Radiological Materials Characterization," *INMM 63rd Annual Meeting*, 2022.

[5] Venkataraman, R., et al. *Gamma ray Imaging Based Methods to Improve the Accuracy of Uranium Holdup Quantification*. No. IROS18159. Oak Ridge Y-12, 2020.

[6] Preston, J., et al. *Uranium Holdup Monitoring with Compton Imaging as Function of Depth and Mass*. No. IROS37367. Oak Ridge Y-12 Plant, 2021.

[7] Ziock, K. P., and M. A. Blackston. "Real time depth-of-interaction correction for coded-aperture, gamma-ray images." *Nuclear Instruments and Methods in Physics Research Section A: Accelerators, Spectrometers, Detectors and Associated Equipment* 916 (2019): 56-65.